JOURNAL OF MATERIALS RESEARCH AND TECHNOLOGY 2021;15:5623–5634

Available online at www.sciencedirect.com

jmr&t Journal of Materials Research and Technology

journal homepage: www.elsevier.com/locate/jmrt

Original Article

Comparative study of finishing techniques for age-hardened Inconel 718 alloy

Jon Ander Sarasua Miranda [a,*], *Ander Trinidad Cristobal* [a], *Haizea González-Barrio* [b], *Pablo Fernández-Lucio* [b], *Gaizka Gómez-Escudero* [b], *Aitor Madariaga* [c], *Pedro Jose Arrazola* [c]

[a] *Tekniker, Spain*
[b] *Universidad del País Vasco (UPV/EHU), Spain*
[c] *Mondragon Unibertsitatea, Spain*

ARTICLE INFO

Article history:
Received 6 July 2021
Accepted 4 November 2021
Available online 11 November 2021

Keywords:
Nickel-based alloy
Polishing
Burnishing
Hammer peening
Surface integrity

ABSTRACT

Inconel 718 is a widely used alloy in the aeronautic sector due to its excellent mechanical and corrosion wear resistance under high temperature conditions. However, its good mechanical properties can be a double edge sword in terms of manufacturing, especially in those processes based in mechanical principles, such as machining or forming. Considering that most aeronautic components are exposed to cyclic load and temperature, fatigue resistance becomes critical, and therefore, the finishing processes. The surface integrity of a component plays an important role on its fatigue behaviour, as the most common crack initiation area is usually the surface. The present work compares three different mechanical finishing processes that confer better surface properties to the component: polishing, burnishing, and hammer-peening. Each one achieves different degrees of roughness, and residual stress on the surface. The study is not only focused on the resultant mechanical properties, but also in productivity and process robustness. It is concluded that each technology excels in a different property.

1. Introduction

The air transport has increased significantly since its first commercial flight, and the improvement of aeroengines has been one of the key factors on that evolution. The implementation of new materials with excellent mechanical and chemical properties at high temperatures has allowed this improvement [1]. The nickel-based alloys have been the most employed in critical aero-engine components subjected to high mechanical loads and temperatures [2], and especially the superalloy Inconel®718 has been widely employed for the manufacturing of aero-engine parts [3].

Inconel®718 is a nickel-based alloy, well known in the machining sector as a hard-to-process material. Its low thermal conductivity and work-hardening behaviour are the main responsible of generating high cutting loads and temperatures, that accelerate tool wear and affect the surface integrity (SI) of

* Corresponding author.
E-mail address: jonander.sarasua@tekniker.es (J.A. Sarasua Miranda).
https://doi.org/10.1016/j.jmrt.2021.11.024

the final component [1,4]. In fact, if machining processes are not correctly selected, the SI (which includes microstructural damage, surface roughness, hardness changes and residual stresses) can be adversely affected, and therefore dramatically reduce the performance of the final component. Bearing in mind the strict requirements of the aeronautical sector, machined Inconel®718 components must undergo critical finishing operations that confer them the final properties. The most common finishing processes are based in the combination of indentation (shot-peening, burnishing, hammer peening ...) and abrasive (grinding, polishing, lapping ...) principles.

Shot peening is based on blasting the surface of a component with solid particles. These particles can be made of steel, ceramic or glass, and each of them acts like a tiny shot producing a small indentation in the surface. The application locally yields the material inducing beneficial residual compressive stresses, which depend on the base material and component design. To obtain these benefits, Zhao et al. [5] reached the conclusion that the most important parameters to control are surface coverage and the Almen intensity. Nakamura et al. [6] showed that under the same fatigue cycles, the strain range of shot peening Inconel®718 was 1.3 times that of the polished sample under strain controlled axial fatigue. Importantly, compressive residual stress can delay the crack initiation, but its effect can be relaxed depending on the magnitude of cyclic loads and temperature as observed by Hoffmeister et al. [7,8]. Other authors [9,10] showed that shot-peened Inconel components have better performance, reduced maintenance and provide a cost-effective solution to premature failure in critical components.

Hydrostatic ball burnishing is a non-material removal operation, where a ceramic or hard metal ball roles over a surface under a certain pressure to improve surface quality, so it can be classified as indentation related finishing operation. By means of this plastic deformation, the surface material is displaced in cold so that the peaks of surface roughness fill the hollows of the valleys, achieving better surface roughness results [11]. However, the main advantage of this technique resides on the generation of compressive residual stresses, which improve the mechanical fatigue resistance. This means a better behaviour during service life and performance for components subjected to high loads during many work cycles, such as the blades made of Inconel®718 of the aeronautical engine low-pressure turbine [12]. The correct implementation of hydrostatic ball burnishing lies on the knowledge of the influence of the process parameters in the final component. An example of this was shown in the study performed by Saldaña-Robles et al. [13] in which changing the values of burnishing parameters achieved an improve of more than 80% in the surface roughness or a 14% hardened surface. In line with this, Hua et al. [14] stated that an increase of 15% in surface hardness means an improvement of 83% in mechanical fatigue failure in Inconel 718 components. Applying the correct burnishing parameters, components life can be improved. Therefore, burnishing is widely used in railroad industries or in die and mould sector, among others, especially for components that must withstand high cyclic loads during their service life.

Within indentation-based techniques, machine hammer peening (MHP) with guided tools is a relatively new mechanical surface treatment. This technique is gaining more importance in industrial applications for improving fatigue performance or corrosion resistance of structural parts or surface roughness of dies [15]. During continuous contact machine hammer peening process, the tool is initially moved down a distance z0 (initial offset), and then, the head of tool advances in the main direction at feed of v and impacts the surface of the part with a f hammering frequency. To treat the entire surface, the tool describes linear or curved tool paths separated with a stepover distance of s. Chen et al. [16] studied the effect of MHP on the surface integrity of an oil-graded Inconel®718. They found that for the tested conditions, hammer peening increased the hardness to the depth of about 1000 μm, induced compressive residual stresses (around −730 MPa at the surface) and reduced the roughness induced previously by machining from 23 μm to 9 μm. The induced surface integrity improved the corrosion resistance as it is explained in greater detail by the same authors [17]. More recently, Trauth et al. [18] analysed the influence of MHP on the surface integrity and fatigue performance of surface previously cut by wire electro discharge machining (wire EDM). They demonstrated that the surface was smoother, harder and with more compressive residual that the one produced by EDM. Furthermore, MHP increased the fatigue strength by a factor of approximately 1.4 compared with wire EDM.

With regards to abrasive finishing methods, grinding is one of the oldest ones, so the specific case of Inconel®718 has already been extensively studied for diverse scenarios. Yao et al. [19] investigated how it affected the surface integrity of Inconel®718 components after grinding with vitrified bond single alumina wheel and a resin cubic boron nitride wheel. Rodrigo de Souza Ruzzi et al. [20] studied how surface topography is affected depending on the different cutting parameters involved in grinding, where they concluded that the parameters that most affected surface finish were wheel speed and depth of cut. Many other research focused on the wear of the wheel, e.g., Rao et al. [21] analysed the effect of wear behaviour of single- and poly-crystalline CBN grains on the grinding performance of Inconel®718. Other authors have studied more particular cases, such as the effects of open pores on grinding performance of Ti–6Al–4V alloys [22] analysing grinding forces, force ratio, ground surface roughness and microhardness parameters, or the vibration coupling effects in two different directions and machining behaviour of ultrasonic vibration plate device for creep-feed grinding of Inconel 718 [23], seeing the differences between the real experiments and finite element method and the apparent elastic method.

Polishing is also based in abrasive tools, but they are usually made of elastic and soft based materials, so that the process does not modify the macroscopic geometry of the component. This is a widely used manual method, not only in aeronautics, but also automotive and mould and matrix sectors. The abrasive grains of the polishing disc behave as micrometrical cutting edges that remove very thin layers of the material. This is, therefore, one of the last mechanical manufacturing processes of a production chain. Polishing is

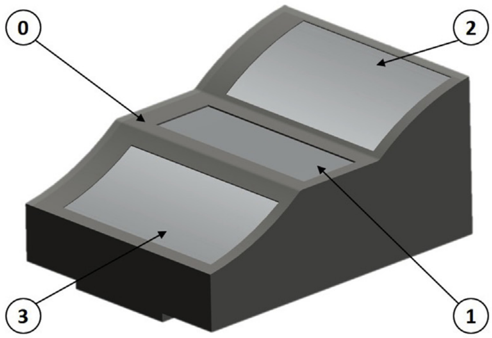

Reference zone:	EDM	0
Flat zone	Hammer Peening	1
Convex zone	Robot Polishing	2
Concave zone	Hydrostatic ball Burnishing	3

Fig. 1 – Test piece and different zones.

still done manually, so reliability and repeatability are not comparable with other controlled processes such as grinding. Parameters such as force (pressure) or feed are not controlled, so many researchers focused their studies in keeping the process variables constant during the operation. Wang [24] and Tian [25] stated that maintaining a constant force during the polishing of flat or constant curved surfaces improves dramatically the treated surface quality. However, this approach turns challenging for complex surfaces. Wang [24] suggested a collaboration between robots and workers, where the robots provide precision, strength and constancy, and the worker provides adaptability, expertise and decision-making power. According to Nagata [26] the stiffness of the machine may be another significant issue. While the CNC machines provide good stability and rigidity to the process, the robotic arms might suffer from dynamical instabilities. However, Wang [24] concluded that the lack of stiffness of the robot does not influence the quality of the component significantly. Wan [27] asserted that the combination of 6 degrees of freedom and low process forces, makes the robotic arm appropriate for the polishing task. In terms of pressure, the ideal thresholds should be in between 7 and 14 kPa [28]. Although it seems to be a light pressure in a macroscopical sight, due to the interaction of the microscopical abrasive particles, the contact forces are high enough to remove material. The force applied by each one of the particles determines the process temperature as well as the number of plastically deformed layers, resulting in the visual and mechanical quality of the component.

As it is shown, the state of the art of finishing processes is based on isolated results that cannot be compared with each other, as the initial state of the samples (material, grain size, roughness, hardness ...) are completely different from one to another. With the aim of increasing the knowledge of finishing processes, the novelty of the present work resides on comparing three controlled processes (polishing, burnishing and hammer-peening) for the same sample material. The

Fig. 2 – 5-axis Kondia HS1000 machining center and Ecoroll Hydraulic pump.

Table 1 – Process parameters used Burnishing.

Feed (mm/min)	Pressure (MPa)	ae (mm)
2000	30	0.05

comparison is done in terms of surface integrity (roughness and residual stresses), and productivity, so that not only the quality aspect of the process is considered, but also the economic ones. Additionally, the case study proposed in this work, suggests the possibility to combine different techniques depending on the specifications of each surface.

2. Experimental procedure

2.1. Materials

Firstly, to carry out the surface finishing tests, a square block of age hardened Inconel®718 of 45 HRC hardness was used, which was cut by electro discharge machining (EDM) in order to generate different curved and flat geometries to apply those operations. Specifically, three different zones were defined, one flat (1), one concave (2) and other convex (3), being the radius of curvature of 150 mm on both curved surfaces. As it will be later explained, the polishing and the burnishing processes were performed on the curved surfaces, as the equipment consisted of a 5-axis machine and a robotic arm. The hammer peening equipment was assembled on a 3-axis machine, so only flat surfaces could be treated under this configuration. The Fig. 1 shows the different test zones. All the process parameters were previously optimized starting from tool providers recommendations and reaching the best integrity balance (best residual stress and roughness).

2.2. Burnishing

The burnishing process was carried out on a Kondia HS1000 5-axis machining centre with a power of 18 kW and spindle locking capability, which is a necessary requirement for hydrostatic ball burnishing (Fig. 2). For this process, a special burnishing tool was used with a 6 mm diameter ceramic ball (HG6-19E90-ZS20-X) as well as a hydraulic pump HGP 6.5 Ecoroll. The area tested with this operation was the concave area where a 5-axis operation was programmed to perform the surface finish. The selected burnishing parameters were obtained from previous tests on a test piece, varying the pressure between the contact of the burnishing ball and the

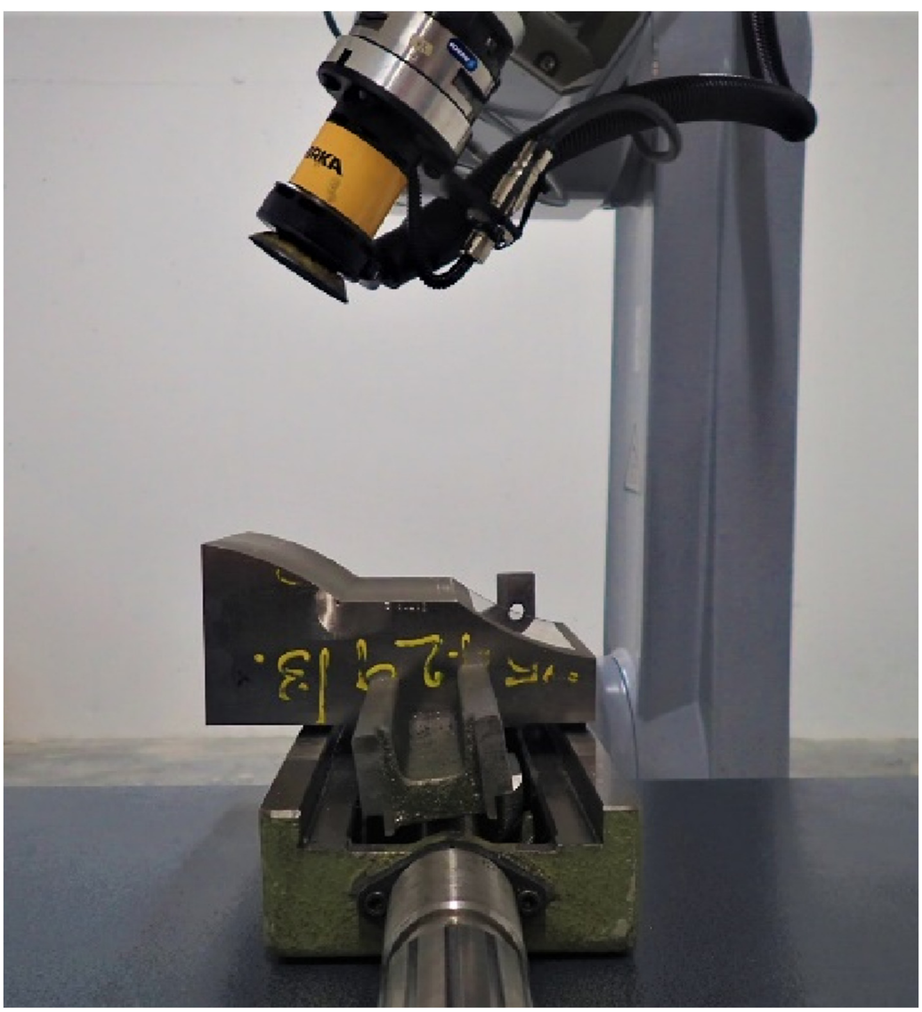

Fig. 3 – Robotized polishing cell.

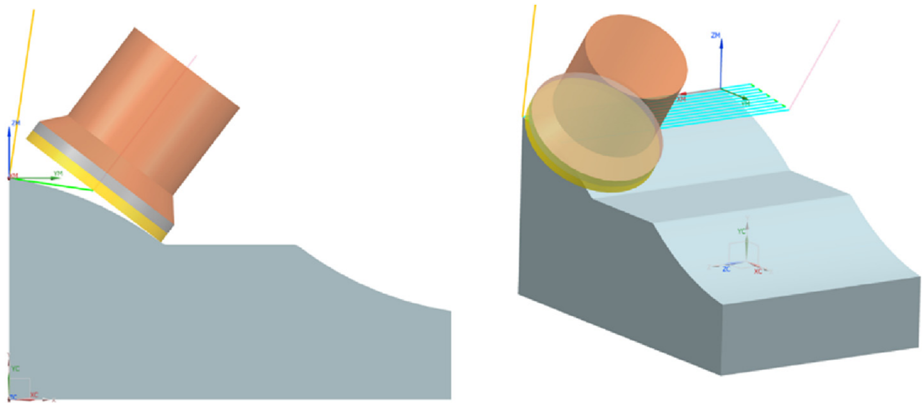

Fig. 4 – CAM polishing trajectories.

contact surface and the distance between consecutive passes aka radial depth of cut (ae). In said experiments, pressures between 10 and 30 MPa and radial depths of cut between 0.05 and 0.10 mm were tested. It was found that there was an ideal pressure and radial depth of cut for a given feed speed, 1000 mm/min concretely (Table 1).

The burnishing trajectories have been programmed in the NX CAM module due to the complexity of the surface, which is a concave surface, and the need for the path to maintain a normal orientation along the path between the surface and the tool to ensure constant pressure.

2.3. *Polishing*

The polishing cell (Fig. 3) is based on a Stäubli rx160 industrial robot, a Schunk FTN-Delta SI-165-15 force sensor and a Mirka Airos 350CV 77 m polishing head all connected to a Beckhoff PLC through a Beckhoff Stäubli project with the NCI interpreter module implemented which confers the robot the possibility of moving the 6 DOF using G-code.

The trajectories were programmed in NX CAM module, since the force sensor adjusts the trajectory to maintain a constant pressure, the accuracy is not an important parameter. Although the trajectory does not need to be so accurate, in order to achieve a homogeneous finish every millimetre needs to be treated. Due to the curved part surface and planar headed polishing surface the generation of the trajectory becomes a bit complex, making necessary to constantly adjust the incidence angle along a trajectory drawn on a plane as shown in Fig. 4 so that all the spaces get treated.

For the polishing of the Inconel®718 part, an empirical model was used to determine the most adequate process parameters shown in Table 2. The input parameters were initial average roughness (Ra) and the final desired R_a. The model gave back the process parameters for each one of the sandpaper grades (P80, P320 and P800) along with an accurate final roughness prediction.

- Pushing force *P* [N]
- Feed *F* [mm/min]
- Number of passes *n* [-]
- Spindle speed S [rpm]

With the aim of improving the visual result and surface quality result, an additional pass with a P1000 cloth was also included in the process.

2.4. *Hammer peening*

The hammer peening tests were performed in a CNN Kondia B1050 machine. A FORGEfix pneumatic hammer peening tool with a cemented carbide indenter (diameter of 20 mm) was assembled in the tool holder of the CNN machine. To select the final testing conditions preliminary tests were done in a rolled sheet of age-hardened Inconel®718. In all preliminary tests the tool was moved down an initial offset (Z_o), ii) then the tool moved from the left to the right at constant feed (*v*) and hammering frequency (*f*), iii) at the end of the path, the tool was raised and moved back to the initial position and iv) finally, the process was repeated once moving laterally the stepover distance (*s*). The feed, hammering frequency and air supply (≈6 bar) were kept constant in these preliminary tests. A total of four conditions were tested using the parameters shown in Table 3.

Table 2 – Process parameters used on the Incone®718 part.

	P80	P320	P800
P [N]	30	20	10
F [mm/min]	300	300	300
n [-]	8	6	4
S [rpm]	7000	7000	7000

Table 3 – Process parameters used in the preliminary hammer peening tests.

Test	*v* (m/min)	s (mm)	Zo (mm)	f (Hz)
1	5	0.07	0.5	≈250
2	5	0.35	0.5	≈250
3	5	0.07	1	≈250
4	5	0.35	1	≈250

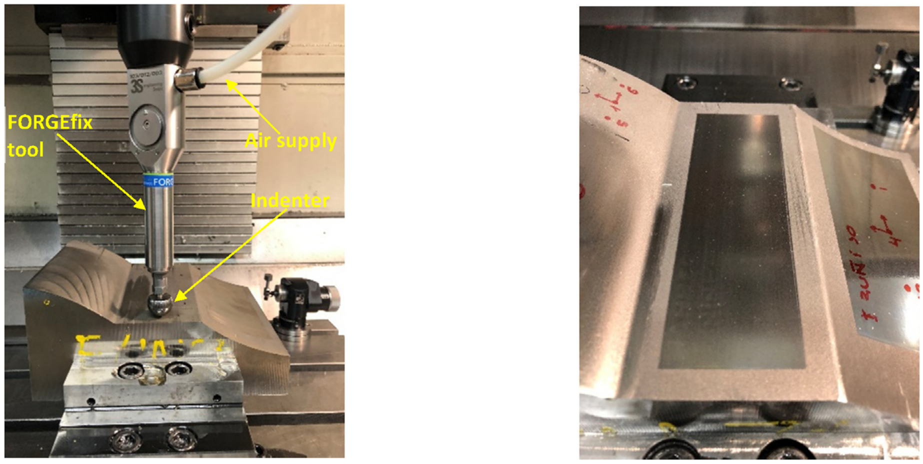

Fig. 5 – Set-up for the hammer peening tests (left) and final surface (right).

To select the best process conditions residual stresses were measured (unpublished work). The conditions used in Test 2 produced the higher compressive residual stresses and therefore, these were used to carry out the final tests in the flat surface of the Inconel®718 part. This part was fixed in the same CNN machine, and it was hammer peened with the same FORGEfix tool (see set-up in Fig. 5). It should be clarified that the feed direction was along the width of the part, the longest side of the flat surface.

2.5. *Surface integrity characterisation*

Initially, surface residual stresses were measured non-destructively in the curved and flat surfaces of the part by the X-ray diffraction method prior to applying the three surface finishing techniques. A Bruker D8 advance diffractometer was used for this purpose. The radiation employed was CrKα1 (λ=2.291 Å), with voltage of 40 kV and current of 40 mA. The (2 2 0) diffraction plane of the austenitic matrix was chosen for the measurements. A round collimator (2 mm diameter) on the incident beam was used. Measurements carried out in Ω mode with 9 inclinations and experimental data were analysed by means of Diffrac software. Diffraction peaks were fitted with a Pearson VII function that is necessary for eliminating errors from varying blending and defocusing of the Kα doublet diffraction peak [Prevey 1986]. The diffraction elastic constants used in the measurements were the following: $-S_1 = 1.500 \cdot 10^{-6}$ [MPa^{-1}], ½ $S_2 = 6.500\ 10^{-6}$ [MPa^{-1}].

The residual stresses generated in the surfaces treated by the three processes were measured using the Hole-Drilling technique. For that purpose, an MTS Restan 3000 an equipment was used (see Fig. 6, left). Strain gauges CEA-062UL-120 were glued at the measurements points as shown in Fig. 6 following the specifications given by the gauge supplier Vishay. The drill bit of diameter 1.6 mm was aligned with the gauge before drilling the hole. The zero depth was detected by electrical contact between the drill bit and the surface of the part. Subsequently, the fine incremental hole drilling procedure [29] was done at each measurement point using a total of 15 depth increments: five initial increments of 20 μm, the next six increments were of 50 μm, and finally four increments of 100 μm. This procedure made a hole of ≈1.8 mm diameter and a depth of 800 μm. During the tests, strains were recorded in a HBM data acquisition system after finishing each increment. Finally, the residual stress profiles were calculated as described in the ASTM-E357 standard.

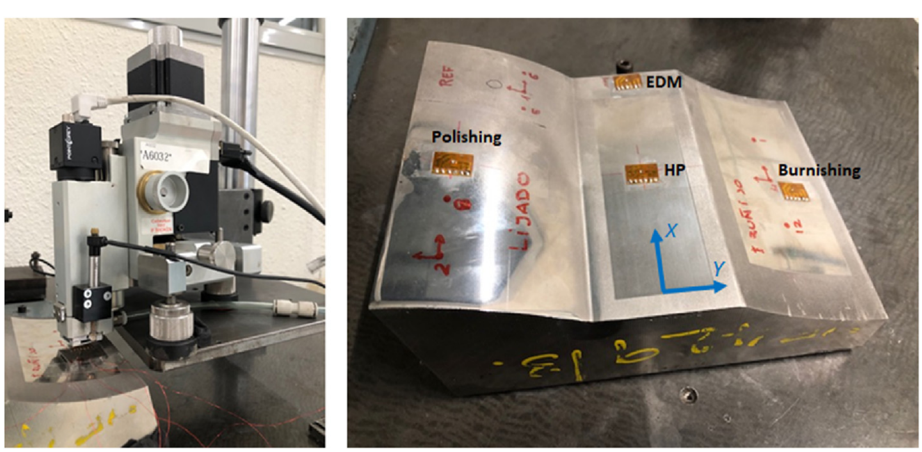

Fig. 6 – Set-up for residual stress measurements (left) and identification of measured points (right).

In terms of surface topography, a confocal optical microscope with a resolution of 0.1 nm was used, concretely, a Leica DCM3D microscope (see Fig. 7). Roughness measuring setting, in this case, was an evaluation length of 4 mm and a 0.8 mm cut-off length for each zone, according to the standard of ISO 4288 [15].

3. Results and discussion

With the aim of evaluating obtained surfaces using the three different processes, residual stresses, roughness, topography and productivity results were analysed in detail in the following subsections. In addition, Fig. 8 shows the final part after all the finishing processes.

3.1. *Residual stresses*

The initial surface residual stresses after EDM process measured by the X-ray diffraction technique in the width direction of the curved and flat surfaces are shown in Fig. 9. In general, low tensile residual stresses (ranging from 60 to 125 MPa) were induced and therefore slight differences can be appreciated between the different surfaces. The flat area turns to be the most tensile one, which can be related to the fact that during a linear cut, the EDM wire increases the linear speed, and therefore, the material removal rate. In any case, the differences between the initial values are neglectable compared to the effect of each finishing process and also to the yield stress of the material (≈1180 MPa at room temperature).

Figure 10 shows the residual stress profiles measured in each of the surfaces after the finishing processes. Importantly,

Fig. 7 – Set-up for roughness and topography measurements.

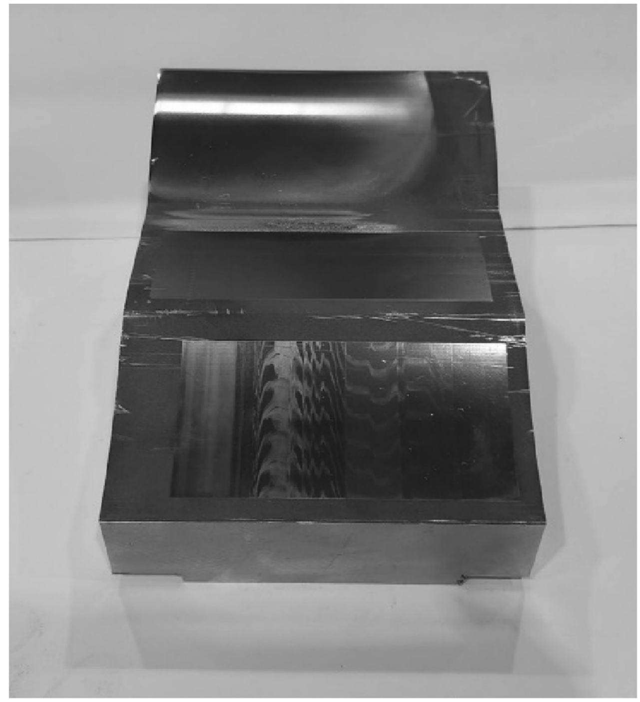

Fig. 8 – Final state of the whole sample.

the burnishing and hammer peening process induced high compressive residual stresses near and beneath the surfaces in both x and y directions. The polishing process did not modify significantly the initial residual stress state. It was able to remove slightly the tensile residual stresses locked near the surface and generate slightly more compressive residual stresses beneath the surface. In fact, the forces applied during polishing were very low compared to the other two mechanical treatments and therefore it seems reasonable to have a lower impact on the residual stress profile beneath the surface.

The burnishing process induced a higher compressive residual stress and thicker compressed layer than the hammer peening process. During the burnishing process an ideal pressure of 30 MPa was applied to the device, while the hammer peening process applied a pressure of 0.6 MPa (6 bar). Additionally, the diameter of the sphere used in the ball burnishing processes was three times lower than the indented used in the hammer peening process. Based on Hertzian contact theory, these processes conditions clearly induce higher contact pressures in the burnishing processes than in the hammer peening processes, leading to 250–500 MPa more compressive residual stresses (at depths >300 μm) and a thicker compresses layer.

However, the hammer peening process induced very high residual stresses near the surface. These high compressive residual stresses are higher in the X direction (main motion of the tool), even above the yield stress of the bulk material ($\sigma y = 1180$ MPa). This means that the surface layer was work-hardened and therefore the yield stress of the surface layer increased. During the hammer peening process, the indenter slides along the surface, generating high friction forces since the pressure is high. These friction forces stretch plastically the surface layer and high compressive residual stresses are

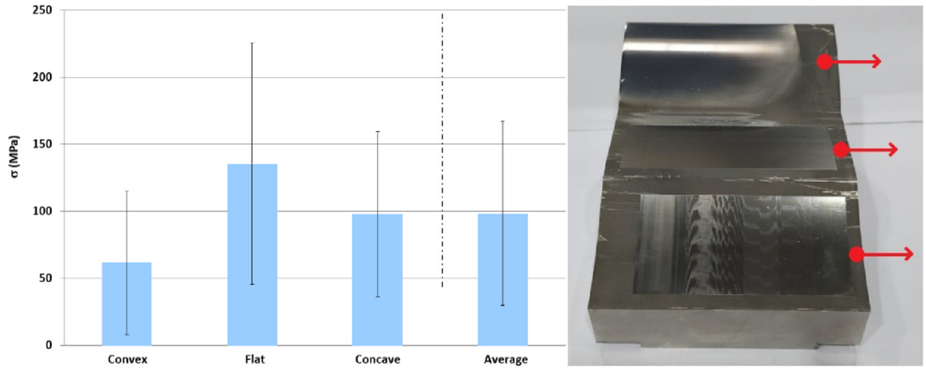

Fig. 9 – Initial residual stress values (left) for each measurement points (right).

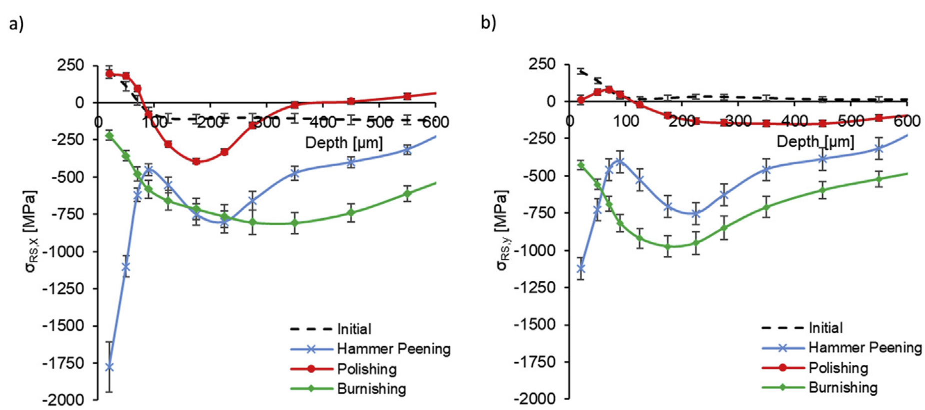

Fig. 10 – Residual stress profiles in a) the x direction and b) the y direction.

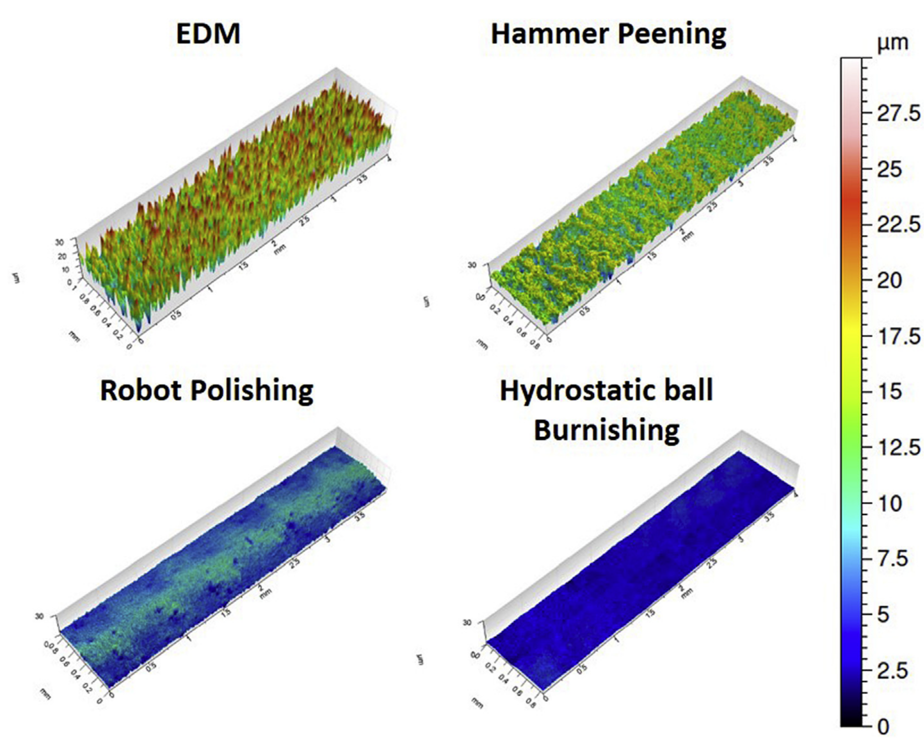

Fig. 11 – Surface topographies of the different finishing techniques.

Table 4 – Surface topographies height parameters.

ISO 25178								
Height Parameters								
	EDM		Hydrostatic burnishing		Hammer Peening		Robot Polishing	
Sa	3.81	μm	0.386	μm	2.49	μm	1.45	μm
Sz	29.8	μm	4.94	μm	21.0	μm	10.8	μm
Sq	4.81	μm	0.491	μm	3.04	μm	1.86	μm
Sp	16.0	μm	2.36	μm	8.32	μm	5.55	μm
Sv	13.8	μm	2.59	μm	12.7	μm	5.27	μm

generated to reach the balance once the process is finished. Furthermore, these additional local plastic deformation produces a work-hardened layer. In contrast, the ball rolls on the surface of the workpiece during the burnishing process, and therefore the friction forces are minimal. Consequently, no additional compressive surface residual stresses are induced. In summary, the compressive residual stresses induced by ball burnishing are mainly produced by the hertzian contact, while the residual stresses generated by hammer peening are due to the combination of contact pressures and friction forces.

3.2. *Roughness and topography*

With the application of any of the finishing techniques, an improvement in the surface roughness was obtained compared with the reference, which in this work is an EDM cut surface. These results are shown in Fig. 11 and Table 4. The first one shows the 3D topography of a selected area of each zone of the part, being the dimensions of 0.8*4 mm^2 approximately. And the second one shows the height parameters values of these topographies. It is noteworthy that with the three of them the peaks resulting by EDM operation were notably reduced. Quantifying these improvements, it is shown that with hydrostatic ball burnishing the surface arithmetical mean of height (Sa) was improved by almost 90%, around 62% with robot polishing and 34.65% with hammer peening. Regarding surface maximum height values (Sz), as with the Sa parameter, the greatest improvements were also achieved with hydrostatic ball burnishing, 83.42%, with an improvement of 63.76% in robot polishing and 29.53% in hammer peening.

In addition, roughness profiles were also extracted. These measurements were carried out 5 times for each zone and Fig. 12 shows a representative measurement of those profiles, along with the table of amplitude parameters, see Table 5, in which the values of Ra and Rz are shown.

3.3. *Productivity*

The productivity of the subtractive processes is usually measured in material removal rate (mm^3/min), which is not applicable to non-subtractive processes. However, polishing is always a finishing operation, so to make a reasonable comparison, it was opted to consider the magnitude of area per time (mm^2/min) as reference. Table 6 shows the areas treated by each of the operations, times, and productivities.

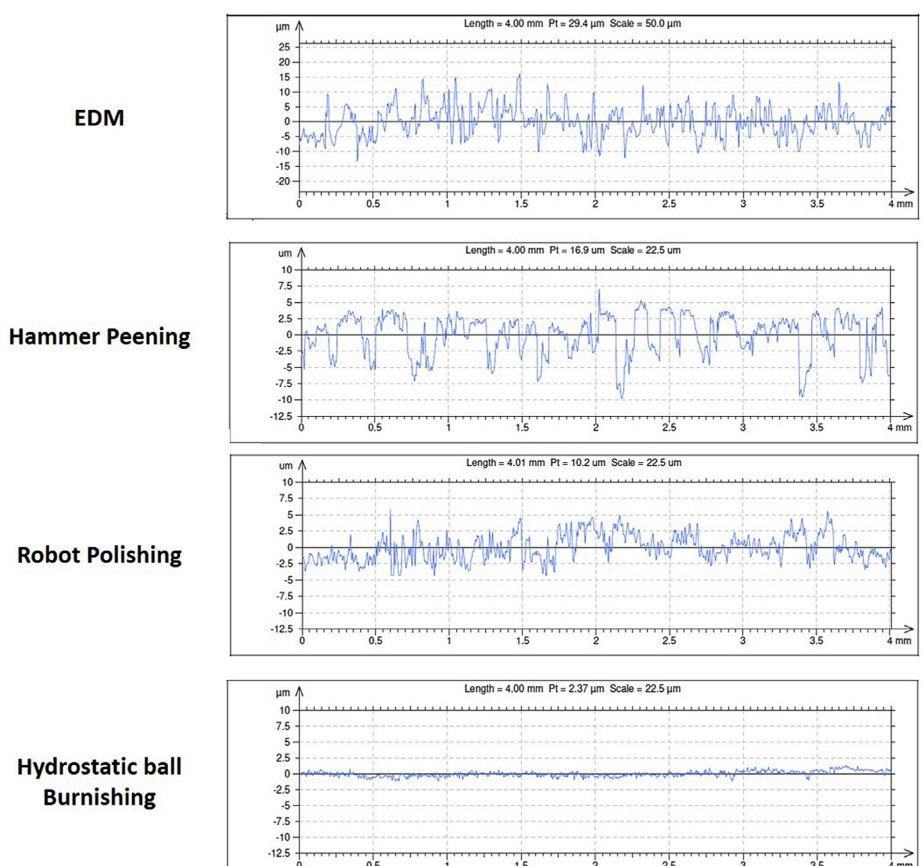

Fig. 12 – Roughness profiles and amplitude parameters.

Table 5 – Roughness profiles amplitude parameters.

ISO 4287								
Amplitude Parameters–Roughness profile								
	EDM		Hydrostatic ball Burnishing		Hammer Peening		Robot Polishing	
Ra	17.00	μm	0.15	μm	12.20	μm	5.66	μm
Rz	2.95	μm	0.75	μm	2.46	μm	1.01	μm
Spacing parameters – Roughness profile								
RSm	0.061	mm	0.025	mm	0.134	mm	0.046	mm
	Gaussian Filter, 0.25 mm		*Gaussian Filter*, 0.08 mm		*Gaussian Filter*, 0.8 mm		*Gaussian Filter*, 0.25 mm	

Table 6 – Productivity ratios of the three different processes.

	Polishing	Burnishing	Hammer peening
Area [mm^2]	7000	6924	5200
Time [min]	7.9	153.2	30.6
Productivity [mm^2/min]	885.7	46.2	170

As shown in Fig. 13, polishing was the most productive process. Even using 4 different abrasives, the productivity was about 20 times higher than burnishing and 5 times higher than hammer peening. The main reason could be attributed to the size of the tool (abrasive disc). Regardless of the feed rate parameter (mm/min), burnishing needed a side pass of 0.05 mm and for the case of hammer peening, around 0.35 mm. Polishing used a side pass of 10 mm, covering the whole area with fewer passes, even having to repeat the same procedure for several grain sizes.

Each studied processes outperformed in one field, but with a significant drawback:

- Hammer peening generated the most compressive residual stresses near the surface but gave rise to the highest roughness.

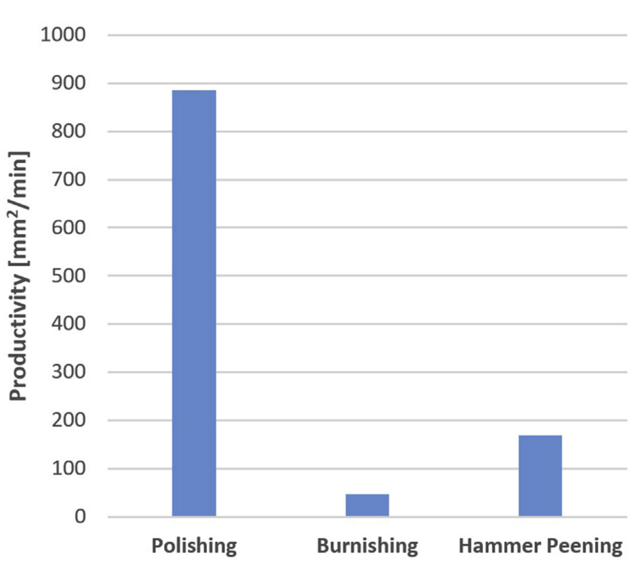

Fig. 13 – Productivity ratios of each process.

- Burnishing obtained the best roughness and the thickest compressive layer, but with the lowest productivity.
- Polishing was the most productive process, but practically there was no significant compressive residual stress enhancement.

Figure 14 summarizes the mentioned advantages and drawbacks.

From the industrial point of view, the aeronautical sector is characterized by its strict requirements in terms of surface finish and integrity. In this sense, hammer-peening and burnishing techniques would be the most suitable. However, hammer peening obtained not optimal roughness and burnishing was not sufficiently productive. Polishing, on the other hand, obtained an acceptable roughness and it was very productive, but it was not able to improve the surface properties. Thus, it is demonstrated that none of the finishing technologies studied reaches an adequate compromise. However, the combination of technologies could be a possible solution to enhance the advantages and reduce the problems. In this way, depending on the main component requirements, the following combinations could be made:

- General compromise: hammer peening + polishing.
- Very high quality for high added value components: hammer peening + hydrostatic ball burnishing

Another possible option would be to focus each process on certain applications. Depending on the specific

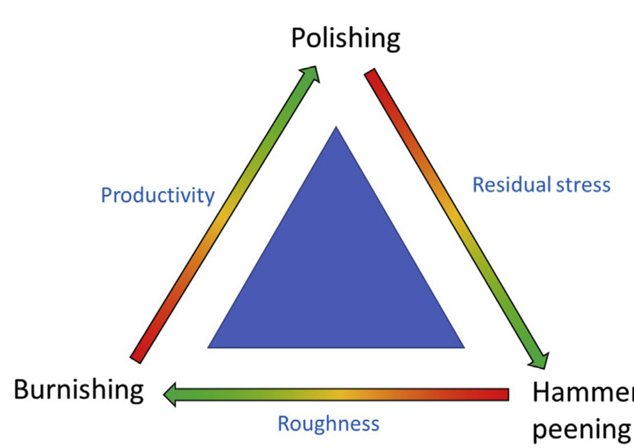

Fig. 14 – General comparison between processes.

requirements of each surface, each of the techniques can be suitable. For instance, if a smooth surface is required but residual stresses are not critical, polishing is the best choice. However, if compressive residual stresses and low surface roughness are required, burnishing would be the most appropriate one.

4. Conclusions

This paper has compared the productivity and the effect of three finishing processes on the surface integrity generated in the nickel-based alloy Inconel®718. The main conclusions are described below:

- Pneumatic hammer peening and ball burnishing generated compressive residual stresses near and beneath the surface which could improve the fatigue and corrosion behaviour of the workpiece. Although pneumatic hammer peening generated very high residual stresses near the surface ball burnishing induced a thicker compressive layer as consequence of the higher applied pressure and the use of a smaller sphere. Polishing slightly affected the residual stress state for the tested range of conditions.
- With the three finishing techniques the surface roughness was improved. By means of hydrostatic ball burnishing excellent roughness values were achieved, between N3 and N4 according to the table of Relation between arithmetical average Roughness (Ra) and Conventional parameters of JIS B 0601 standard. While with polishing they were between N8 and N9, although it could be reached a mirror effect finish surface. Hammer peening slightly improved the surface topography produced by EDM, maybe due to the low pressure used in the process, reaching values close to N10.
- On grounds of higher side pass, the productivity of polishing was higher than ball burnishing and pneumatic hammer peening, that were based on compressing every square mm of surface with a small. Therefore, to treat a 1 m^2 surface, it would take 98 h of hammer peening and 360 h of ball burnishing, while polishing would take 18 h.
- Each process excels in a certain characteristic, so the balance could be found by combining them or by focusing each one on specific applications.

Declaration of Competing Interest

The authors declare that they have no known competing financial interests or personal relationships that could have appeared to influence the work reported in this paper.

Acknowledgements

This work was financially supported by the "Desarrollo Económico e Infraestructuras" department of the Basque Government (ELKARTEK program, project PROCODA KK-2019/00004).

REFERENCES

[1] Ezugwu EO. High speed machining of aero-engine alloys. J. Brazilian Soc. Mech. Sci. Eng. 2004;26(1):1–11.
[2] Miller S. Advanced materials mean advanced engines. Interdiscipl Sci Rev 1996;21(2):117–29.
[3] Loria EA. The status and prospects of alloy 718. JOM 1988;40(7):36–41.
[4] Ulutan D, Ozel T. Machining induced surface integrity in titanium and nickel alloys: a review. Int J Mach Tool Manufact 2011;51(3):250–80.
[5] Zhao C, Gao Y, Guo J, Wang Q, Fu L, Yang Q. Investigation on residual stress induced by shot peening. J Mater Eng Perform Mar. 2015;24(3):1340–6. https://doi.org/10.1007/s11665-014-1382-0.
[6] Hiroshi N, Masahiro T, Yu I, Hiroshi K, Yusuke U. "Shot peening effect on low cycle fatigue properties of TI-6AL-4V and inconel 718. In: Proceedings of the ASME turbo expo, vol. 4; May 2011. p. 791–7. https://doi.org/10.1115/GT2011-46847.
[7] Hoffmeister J, Schulze V, Wanner A, Hessert R, Koenig G. Thermal relaxation of residual stresses induced by shot peening in IN718. In: Proceedings of the 10th international conference on shot peening, tokyo, Japan; 2008. p. 157–62.
[8] Hoffmeister J, Schulze V, Hessert R, Koenig G. Residual stresses under quasi-static and cyclic loading in shot peened Inconel 718. Int J Mater Res 2012;103(1):66–72.
[9] Klotz T, Delbergue D, Bocher P, Lévesque M, Brochu M. Surface characteristics and fatigue behavior of shot peened Inconel 718. Int J Fatig May 2018;110:10–21. https://doi.org/10.1016/j.ijfatigue.2018.01.005.
[10] Chamanfar A, Monajati H, Rosenbaum A, Jahazi M, Bonakdar A, Morin E. Microstructure and mechanical properties of surface and subsurface layers in broached and shot-peened Inconel-718 gas turbine disc fir-trees. Mater Char Oct. 2017;132:53–68. https://doi.org/10.1016/j.matchar.2017.08.002.
[11] Priyadarsini C, Ramana VSNV, Prabha KA, Swetha S. A review on ball, roller, low plasticity burnishing process. Mater Today: Proceedings Jan. 2019;18:5087–99. https://doi.org/10.1016/j.matpr.2019.07.505.
[12] Avilés R, Albizuri J, Rodr\'\iguez A, De Lacalle LNL. Influence of low-plasticity ball burnishing on the high-cycle fatigue strength of medium carbon AISI 1045 steel. Int J Fatig 2013;55:230–44.
[13] Saldaña-Robles A, Plascencia-Mora H, Aguilera-Gómez E, Saldaña-Robles A, Marquez-Herrera A, la Peña JA. Influence of ball-burnishing on roughness, hardness and corrosion resistance of AISI 1045 steel. Surf Coating Technol 2018;339:191–8.
[14] Hua Y, Liu Z, Wang B, Hou X. Surface modification through combination of finish turning with low plasticity burnishing and its effect on fatigue performance for Inconel 718. Surf Coating Technol Oct. 2019;375:508–17. https://doi.org/10.1016/j.surfcoat.2019.07.057.
[15] Schulze V, Bleicher F, Groche P, Guo YB, Pyun YS. Surface modification by machine hammer peening and burnishing. Cirp Ann. 2016;65(2):809–32.
[16] Chen T, John H, Xu J, Hawk J, Liu X. Effects of hammer peening and aging treatment on microstructure, mechanical properties and corrosion resistance of oil-grade alloy 718. Superalloys 2012 2012:609–14.
[17] Chen X, Yan J, Ren S, Wei J, Wang Q. Microstructure and mechanical properties of Ti–6Al–4V/Al1060 joints by ultrasonic-assisted brazing in air. Mater Lett 2013;95:197–200.
[18] Trauth D, Klocke F, Welling D, Terhorst M, Mattfeld P, Klink A. Investigation of the surface integrity and fatigue

strength of Inconel718 after wire EDM and machine hammer peening. Int J Material Form 2016;9(5):635–51.
[19] Yao CF, Jin QC, Huang XC, Wu DX, Ren JX, Zhang DH. Research on surface integrity of grinding inconel718. Int J Adv Manuf Technol Mar. 2013;65(5–8):1019–30. https://doi.org/10.1007/s00170-012-4236-7.
[20] Ruzzi R de S, de Paiva RL, da Silva LRR, Abrão AM, Brandão LC, da Silva RB. Comprehensive study on Inconel 718 surface topography after grinding. Tribol Int Jun. 2021;158:106919. https://doi.org/10.1016/j.triboint.2021.106919.
[21] Rao Z, Xiao G, Zhao B, Zhu Y, Ding W. Effect of wear behaviour of single mono- and poly-crystalline cBN grains on the grinding performance of Inconel 718. Ceram. Int., Mar. 2021. https://doi.org/10.1016/j.ceramint.2021.03.012.
[22] Zhao B, Ding W, Xiao G, Zhao J, Li Z. Effects of open pores on grinding performance of porous metal-bonded aggregated cBN wheels during grinding Ti–6Al–4V alloys. Ceram Int 2021;47(22):31311–8.
[23] Yang CAO, Yejun ZHU, Wenfeng D, Yutong QIU, Lifeng W, Jiuhua XU. Vibration coupling effects and machining behavior of ultrasonic vibration plate device for creep-feed grinding of Inconel 718 nickel-based superalloy. Chinese J. Aeronaut.; 2021.
[24] Wang K (Brian), Dailami F, Matthews J. Towards collaborative robotic polishing of mould and die sets. Procedia Manuf. 2019;38:1499–507. https://doi.org/10.1016/j.promfg.2020.01.137.
[25] Tian F, Lv C, Li Z, Liu G. Modeling and control of robotic automatic polishing for curved surfaces. CIRP J. Manuf. Sci. Technol. Aug. 2016;14:55–64. https://doi.org/10.1016/j.cirpj.2016.05.010.
[26] Nagata F, Hase T, Haga Z, Omoto M, Watanabe K. CAD/CAM-based position/force controller for a mold polishing robot. Mechatronics May 2007;17(4–5):207–16. https://doi.org/10.1016/j.mechatronics.2007.01.003.
[27] Wan YH, Wang G. Polishing robot: status and outlook. Adv Mater Res 2009;69–70:311–5. https://doi.org/10.4028/www.scientific.net/AMR.69-70.311.
[28] Bulsara VH, Ahn Y, Chandrasekar S, Farris TN. Mechanics of polishing. 1998.
[29] Grant P, Lord J, Whitehead P, Fry AT. The application of fine increment hole drilling for measuring machining-induced residual stresses. Appl Mech Mater 2005;3:105–10.